In Situ X-Ray Standing Wave Study of Cu UPD on an Iodine Covered Platinum Surface

G. M. Bommarito, D. Acevedo, J. F. Rodríguez and H. D. Abruña*
Department of Chemistry
Baker Laboratory
Cornell University
Ithaca, New York, 14853-1301

ABSTRACT
In situ structural investigations of the underpotential deposition of copper on an iodine covered platinum surface have been carried out using x-ray standing waves generated by specular (total external) reflection and Bragg diffraction. Surface coverage isotherms derived from both electrochemical and x-ray measurements are also compared. The growth mode of the copper ad-layer appears to be strongly influenced by the electrode's surface morphology.

1. INTRODUCTION

The process of underpotential deposition (UPD) of metals has been extensively studied during the past two decades due to its theoretical and practical importance in fields such as electrocrystallization, catalysis, and surface chemistry. Numerous electrochemical and spectroscopic techniques have been utilized to probe the mechanism(s) of formation, and the structural properties of UPD layers [1-3].

Conventional electrochemical techniques have been used to obtain thermodynamic and kinetic information about the UPD process [1-3]. Although electrochemical methods are invaluable in controlling and measuring thermodynamic parameters such as applied potential, charge, and coverage, any structural inferences are always indirect and often model dependent.

Surface sensitive ultra high vacuum techniques have been employed in the study of such systems and much information has been obtained from them [4]. However, the fact that these studies are inherently ex-situ raises some fundamental questions as to their applicability.

Recently, in situ x-ray spectroscopic and diffraction techniques have provided unique atomic resolution structural information about UPD systems [5]. Extended x-ray absorption fine structure (EXAFS) and x-ray absorption near edge structure (XANES) have been widely used to study various UPD systems [6], providing information about the local structure atomic environment and the oxidation state of the adsorbed species. Furthermore, surface x-ray scattering measurements have been used to study the in-plane structure of the UPD layer for specific cases [7]. In addition to these techniques, x-ray standing waves (XSW) have been utilized to probe the electrochemical double layer [8]. In these studies, one can obtain information pertaining to the distribution of species, including the diffuse layer, in a direction normal to the substrate's surface.

We present the results of a series of in situ x-ray standing wave experiments aimed at probing the potential dependent structural nature of the underpotential deposition of copper on an iodine covered platinum surface.

2. THEORETICAL BACKGROUND

X-ray standing waves are generated when coherently related incident and reflected plane waves interfere. During specular reflection (total external reflection) and Bragg diffraction a strong, well-defined standing wave field is generated. In addition, as the angle of incidence θ is scanned across these reflection regimes, there is a change of π in the

relative phase $\nu(\theta)$, causing the nodal and antinodal planes of the standing wave field to move inward in a direction normal to the substrate's surface (we confine our discussion here to the case where the diffraction planes of the substrate are parallel to the surface). Since the relative phase and the standing wave periodicity are known exactly at all angles θ in both the specular reflection and Bragg diffraction regimes, the position of the nodal and antinodal planes in the standing wave with respect to the substrate's surface is also known as a function of θ. Since the photoelectric effect for core electrons is directly proportional, in the dipole approximation, to the electric field intensity at the center of an atom, the emission yield (i.e. the fluorescence yield) from the atoms in an overlayer or a distributed layer of species above the substrate's surface will be uniquely modulated as a function of θ. To calculate this yield (Y), the standing wave electric field intensity $I(\theta,z)$ must be integrated over the entire distribution N(z):

$$Y(\theta) = \int_0^\infty I(\theta,z)\, N(z)\, dz \qquad (1)$$

Traditionally, XSW experiments have been carried out on perfect single crystals of materials such as Ge or Si. However, for reasons previously outlined [9], including large d-spacings and control of the materials employed, we have used Pt/C layered synthetic microstructures (LSM) as both the diffracting structure and the working electrode.

3. EXPERIMENTAL ASPECTS

The experiments were carried out at the Cornell High Energy Synchrotron Source (CHESS), under parasitic conditions (5GeV, 60-100 mA), using the B2 beam line. An x-ray energy of 9.35 keV was selected, with a double-crystal Si(111) monochromator, to excite copper K_α fluorescence. The incident flux was approximately 10^9 photons/s. A Si(Li) solid-state detector was used in conjunction with a spectroscopic amplifier and a histogramming memory module to measure the fluorescence yield.

The electrochemical cell, housed inside an aluminum holder, consisted of a cylindrical Teflon body with feedthroughs for electrolytes and electrode connections. The filling and rinsing of the cell with electrolyte was accomplished with pressurized glass vessels through the fluid feedthroughs. A thin layer of solution (approx. 1-3 μm thick) was trapped between the electrode, and a 6.35μm thick polypropylene film which was held in place by a Teflon ring. All the electrochemical measurements were carried out with the polypropylene film distended by the addition of excess bulk electrolyte into the cell. The thin layer was then restored by removing excess electrolyte. Potential control of the electrode was retained through filling and rinsing stages. All applied potentials are reported with respect to a Ag/AgCl reference electrode.

Solutions were prepared with ultrapure reagents (Aldrich) and pyrolytically distilled water (PDW). Prior to use, solutions were degassed for over 30 min. with high purity nitrogen.

Platinum/carbon LSMs (15 mm by 20 mm) were obtained from Ovonic Synthetic Materials Co. (Troy, MI). The LSMs used had d-spacings of 39.7 Å or 41.4 Å, and consisted of 200 layer pairs of platinum and carbon with platinum as the outermost layer deposited on a 0.015 in. thick Si(111) substrate.

For each XSW scan, the energy-dispersed fluorescence spectrum at a given angular position was recorded into 256 channels of the histogramming memory module. A typical scan consisted of 64 points over angular ranges of 10 mrad and 3.75 mrad for the specular reflection and Bragg diffraction regions respectively, and took approximately 20 min. to complete. Approximately 2 min/point of data were collected for each potential studied.

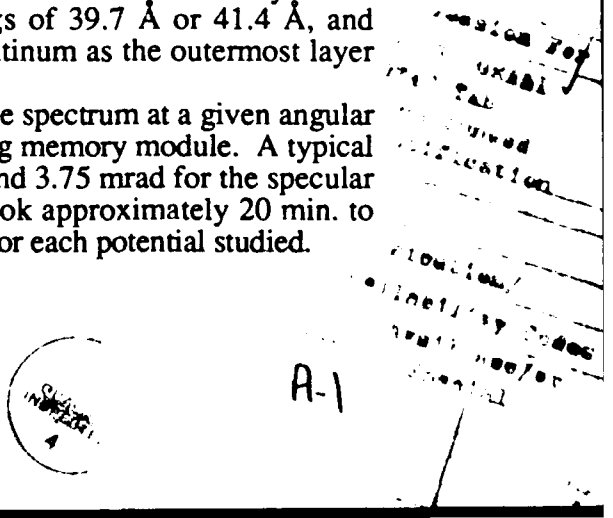

4. RESULTS AND DISCUSSION

A. Electrochemistry

In these experiments, a platinum/carbon LSM was used as the diffracting substrate and working electrode. In sulfuric acid media, the voltammetry due to the platinum surface of the LSM showed only one pronounced (weakly bound) hydrogen adsorption peak. Such behavior has been previously shown to be characteristic of a clean well-ordered (i.e. atomically smooth over long-range) Pt(111) electrode which has been subjected to a few cycles in which a surface oxide layer is formed and removed resulting in a Pt(111) surface with nearly randomly distributed monoatomic steps [10].

We chose to study the underpotential deposition of copper on an iodine covered platinum surface since the latter renders the surface chemically impervious to contamination [11]. In addition, XSW experiments on the electrosorption of iodide on a platinum/carbon LSM had shown that the I ad-layer seems to undergo similar potential dependent structural rearrangements on LSMs as on Pt(111) single crystal electrodes [12]. The UPD of copper on such a surface has been shown to displace the iodine ad-layer and deposit directly onto the platinum surface [11].

Figure 1A shows the cyclic voltammetry (in 0.1 M sulfuric acid containing 0.6 mM Cu(II)) for this system using a platinum/carbon LSM as the working electrode. This voltammetry was obtained after cleaning the electrode surface (i.e. the LSM's surface) by a series of oxidation-reduction cycles at a sweep rate of 20 mV/sec, in pure supporting electrolyte (0.1M sulfuric acid) and forming an iodine ad-layer by placing the clean electrode in contact with an iodide containing solution (1mM sodium iodide in 0.1M sulfuric acid) for approximately 15 min.

A few important points should be made. First, the charge under the cathodic and anodic peaks is equivalent; all of the copper deposited on the surface is removed upon reversing the potential scan. Second, the deposition process can be stopped by holding the applied potential at any value between +0.40 and +0.10 V, resulting in copper surface coverages ranging from 0 to 1 monolayer. Hence, the ability to control precisely and reproducibly the surface coverage. Third, the cyclic voltammetry of copper UPD on a Pt(111) surface which has been oxidized-reduced a few times followed by the adsorption of iodine, is almost superimposable (Figure 1B) to that of the LSM, once again pointing out the structural similarities between these two types of surfaces.

The x-ray measurements were carried out while holding the applied potential at either +0.45, +0.25, +0.2, +0.15 or +0.1 V corresponding to copper surface coverages of approximately 0, 1/4, 1/2, 3/4, and 1 monolayer, respectively.

B. Coverage Isotherms

Copper surface coverages were determined from both electrochemical and x-ray fluorescence measurements. Electrochemically, the coverage can be determined by integrating the charge under the cathodic (or anodic) current peak in the cyclic voltammogram (Figure 1A). The charge can be related to a surface coverage assuming that all of the charge is associated with the reduction of copper ions to copper atoms in a two-electron process, that the electrodeposited copper packs in a given surface structure and that the real area of the electrode is known. Whereas the area of the electrode can be experimentally obtained (from hydrogen adsorption), we are assuming that the copper overlayer forms an hcp structure and that the first assumption is valid.

Surface coverage isotherms from two different sets of electrochemical experiments were obtained. In the first set of measurements, the deposited copper layer was stripped from the surface in the presence of bulk copper (no rinsing experiments). Under these conditions, the charge under the deposition and stripping peaks for various surface coverages is equal. In the second set of measurements, the deposited copper layer is stripped after rinsing the electrode three times with clean supporting electrolyte and with no bulk copper present in solution (rinsing experiments). In these experiments we observe a large discrepancy in the cathodic and anodic charge, the anodic peak always representing a

smaller fraction of the charge measured under the cathodic wave. Comparing these isotherms, we observe a loss of deposited copper after rinsing, which is coverage dependent. At full monolayer coverage the loss is only 16% whereas for sub-monolayer coverages of 3/4, 1/2 and 1/4 we observe drastic losses of 47%, 55% and 62%, respectively.

In the x-ray measurements, the coverage isotherms were determined from the off-Bragg fluorescence yield data of the XSW measurements. (Note: Such off-Bragg (i.e. far from the Bragg angle) yield experiments essentially measure all the copper species contained within the thin layer of liquid trapped between the electrode and the polypropylene film window.) We carried out rinsing and no rinsing experiments equivalent to the ones described above. Again, we observe a drastic loss of surface coverage after rinsing the electrode. However, the fractional losses seen in these x-ray experiments are considerably larger than those measured electrochemically. In an attempt to quantify the x-ray derived isotherms they have been plotted on an absolute scale versus the electrochemical ones normalizing the two data sets at only one point: 0.10V, after rinsing (Figure 2). We note that the coverage isotherms for both the x-ray and electrochemical rinsing experiments are in good agreement, but when we compare the results of experiments where the electrode had not been rinsed, the x-ray measurements indicate the presence of a considerable amount of electrochemically inactive copper, above and beyond the bulk copper present in solution. In addition, XSW measurements corresponding to this coverage place this excess copper at the solid/solution interface. Furthermore, even at applied potentials of +0.45 V, where no electrodeposition has yet occurred, we observe an amount of copper equivalent to approximately 2/10 of a monolayer. Finally, we note that the iodine coverage as determined from x-ray fluorescence, is constant throughout the experiment (Figure 2).

C. X-ray Standing Wave Measurements:

In this section we discuss preliminary results from the analysis of the standing wave fluorescence data corresponding to the rinsing experiments discussed above. Specifically, we measured the standing wave profiles for both specular reflection and Bragg diffraction after deposition at potentials of +0.25, +0.20, +0.15 and +0.10 V and rinsing the electrode with clean supporting electrolyte (no copper present in solution) while maintaining potential control over the system at all times.

The background subtracted Cu K_α XSW fluorescence yield was extracted from each fluorescence spectrum (in energy dispersed form) by fitting to a Gaussian on a quadratic background. These data were χ^2 fitted to the theoretical yields calculated from the integral (1) using a Poisson distribution for N(z). The free parameters in these fits were: the distribution's peak position with respect to the substrate's surface, the distribution's FWHM, and a normalizing constant directly proportional to the distribution's area. In addition, XSW data from the specular and Bragg reflection regions were fitted simultaneously.

The theoretical yields were calculated using a computational scheme based on a stratified interface formalism [13] which allows for the inclusion of the solution and polypropylene layers along with the LSM in a single model, having the advantage of being exact by taking both refraction and absorption properly into account. The best theoretical fits are shown as solid lines on Figures 3 and 4.

In specular reflection XSW, the first antinode reaches the surface at the critical angle. At the LSM's critical angle the standing wave period D_c is 100 Å for the LSM used in the experiments at +0.10, +0.20 and +0.25 V (Figure 3), and 120 Å for the LSM used at +0.15 V (Figure 4). Keeping the above discussion in mind, we note that in all cases studied, the Cu fluorescence yield peaks at the critical angle of the LSM. This means that a narrow distribution of copper exists at the LSM surface for all of the potentials

investigated. However, the period of the standing wave in this regime is large and limits the resolution to which we can determine the distribution's position and width.

To improve the resolution we can make use of the XSW measurements in the Bragg regime, where the periodicity of the standing wave is essentially equivalent to the LSM's d-spacing. Referring to the insets of Figures 3 and 4, we observe rather different XSW profiles as a function of applied potential. The expected yield for a random distribution is proportional to (1 + Reflectivity) but in all cases shown here, the fluorescence peak amplitude to background ratio is well beyond this random limit, indicating that the copper distribution is fairly narrow on the length scale of the standing wave period which in this regime is given by the d-spacing of the LSM and is about 40Å for the LSMs employed (see experimental). The changes in the shape of each standing wave profile are representative of changes in the position of this overlayer with potential, although these changes do not appear to be very large since the peak angular position, taken with respect to the Bragg angle, in each standing wave signal is similar. Fitting XSW data generated in the specular reflection and the Bragg diffraction regimes simultaneously, allows us to probe the same distribution of species on two rather different length scales and two different z-scale origins, leading to an unambiguous result.

Figure 5 summarizes the standing wave results in terms of the distribution profiles at each potential studied. In the main panel all distribution profiles are normalized to the same peak intensity, while in the inset each distribution is plotted in terms of its relative area. Also shown is the surface density profile of the LSM on a normalized scale as determined from reflectivity data (not discussed here) and from which we determined a surface roughness of 6.8Å. Note that the origin of the z scale is defined to be where bulk platinum begins.

An especially revealing way of presenting the data is to plot the center of mass (i.e. the z-position where we reach 50% of the total amount of copper) of each distribution as a function of both applied potential and coverage. This is so because the center of mass is dependent on both the peak position and the FWHM in a given distribution. In order to explain the changes we observe in this parameter we need to consider the surface morphology in terms of the Gaussian model we have chosen to use to fit the reflectivity data. This model is illustrated in Figure 6a, where we plot the fractional concentration of surface sites as a function of position along the z-scale (the Gaussian's area is normalized to one). Note that the origin in the z axis corresponds to the one illustrated in Figure 5. In addition, we have sectioned this concentration profile (Figure 6a) into bins with a width approximately equal to the the closest packing distance for platinum (2.26 Å) in order to introduce a finite size effect. If open surface sites were occupied in a random mode, one would expect a homogeneous copper distribution whose center of mass was always at the same z position, namely the center of the Gaussian representing the surface sites concentration profile (i.e. the position with the largest density of open sites). At the opposite extreme, we have a model in which open surface sites are occupied sequentially with the deepest (closest to z=0 Å) ones first. In this case, the center of mass position would vary with the copper surface coverage. Both of these models are plotted, along with the experimental data in Figures 6b,c as a function of potential and coverage, respectively. It is immediately clear that the observed results are in excellent agreement with the model that involves sequential filling of available surface sites with the deepest ones being occupied first. This finding implies that the more favorable surface sites for deposition are the ones closest to the platinum bulk lattice, either because the substrate-deposit interactions are maximized at these sites, or because the interaction with the electric fields present at the interface is greatest at these locations. In addition, deposited copper atoms either diffuse to these positions or the deposition process itself is "catalyzed" by these particular sites.

Furthermore, we should consider whether the nature of the deposition process is coverage dependent, since lateral interactions among deposited atoms might become more important as the coverage is increased, and what structural role iodine might play. It is also unclear what structural effect rinsing the electrode surface with pure electrolyte has on the

UPD layer. It is likely that some structural rearrangement will be triggered by this rinsing procedure. A comparison of the data shown here with results from XSW experiments were the electrode is not rinsed (under investigation at this moment), should provide the answers to these questions.

5. CONCLUSIONS

We have been able to study in situ, the underpotential deposition of copper on an iodine covered platinum/carbon layered synthetic microstructure, using XSWs generated by specular (total external) reflection and Bragg diffraction. The equilibrium structure of the UPD layer after rinsing of the electrode surface with pure electrolyte is one where the deposited copper density is highest for those surface sites closest to the bulk platinum lattice. In addition, we were able to follow potential dependent changes in the copper surface coverage as determined by independent electrochemical and x-ray measurements. We observe a loss of surface coverage upon rinsing, and a good correlation between the electrochemical and x-ray data. However, x-ray derived isotherms, in the case of no rinsing reveal the presence of a large excess of electrochemically inactive copper at the solid/solution interface, when compared to the corresponding electrochemically derived isotherms.

6. ACKNOWLEDGMENTS.

This work was supported by the Army Research Office and the Office of Naval Research. H.D.A is a Sloan Foundation Fellow (1987-1991). D.A. acknowledges a MARC NIH fellowship. J.F.R. is the recipient of a Ford Foundation Fellowship. The authors are grateful for the contributions made by Donna Taylor and Howell Yee.

7. REFERENCES

1 a. Kolb, D.M., in H. Gerisher and C. Tobias, eds., Advances in Electrochemistry and Electrochemical Enginneering, Vol. 11, J. Wiley and Sons, New York, 1978.
b. Adzic, R. Isr. J. Chem. 18, 166, 1979.
c. Adzic, R., in H. Gerisher and C. Tobias, eds., Advances in Electrochemistry and Electrochemical Enginneering, Vol. 13, J. Wiley and Sons, New York, 1985.
d. Juttner, K.; Lorenz, W.J.; Zeit. Physik. Chemie, 122, 163 (1980).
e. Lorenz, W.J.; Hermann, H.D.; Wuthrich, N.; Hilbert, F.; J. Electrochem. Soc., 121, 1167 (1974).
2 a. Schultze, J.W.; Dickertmann, D. Symp. Faraday Soc. 12, 36, (1977).
b. Salvarezza, R.C.; Vasquez Moll, D.V.; Giordano, M.C.; Arvia, A.J. J. Electroanal. Chem. 213, 301, (1986).
c. Parajon Costa, B.; Canullo, J; Vasquez Moll, D.V.; Salvarezza, R.C.; Giordano, M.C.; Arvia, A.J. J.Electroanal. Chem. 244, 261, (1988).
3 a. Schultze, J.W.; Dickertmann, D. Surf. Sci. 54, 489, (1976).
b. Bewick, A.; Thomas, B. J. Electroanal. Chem. 70, 239, (1976).
4 a. Hubbard, A.T.; Accts. Chem. Res., 13, 987 (1980).
b. Yeager, E.B.; J. Electroanal. Chem., 128, 1600 (1981).
c. Ross, P.N.; Surf. Sci., 102, 463 (1981).
d. Kolb, D.M.; Zeit. Physik. Chemie N.F., 154, 179 (1987).
e. Hubbard, A.T.; Chem. Rev., 88, 633 (1988).
f. Beckmann, H.O.; Gerisher, H.; Kolb, D.M.; Lehnpfuhl, G. Symp. Faraday Soc. 12, 51, (1977).
5 Abruña, H. D. ed. "Electrochemical Interfaces: Modern Techniques for In-Sitiu Structural Characterization" VCH, New York, N.Y. 1991
6 a. Abruña, H.D.; White, J.H.; Albarelli, M.J.; Bommarito, G.M.; Bedzyk, M.J.; McMillan, M.J. J. Phys. Chem. 92, 7045, (1988).
b. Tourillon, G.; Guay, D.; Tadjeddine, A. J. Electroanal. Chem. 289, 263, (1990).

c. Tadjeddine, A. J.; Guay, D.; Ladouceur, M.; Tourillon, G. Phys. Rev. Lett. 66, 2235, (1991).
7 a. Samant, M.G.; Toney, M.F.; Borges, G.L.; Blum, L.; Melroy, O.R. J. Phys. Chem. 92, 220, (1988).
b. Toney, M.F.; Gordon, J.G.; Samant, M.G.; Borges, G.L.; Wiesler, D.G.; Yee, D.; Sorensen, L.B. Langmuir 7, 796, (1991).
8 a. Bedzyk, M.J.; Bommarito, G.M.; Caffrey, M.; Penner, T. Science 52, 248, (1990).
b. Bommarito, G.M.; White, J.H.; Abruna, H.D. J. Phys. Chem. 94, 8280, (1990).
9 Abruña, H. D.; Bommarito, G. M.; Acevedo, D. Science, 250, 69 (1990)
10 Aberdam, D.; Durand, R,; Faure, R,; El-Omar, F. Surf. Sci. 171, 303, (1986).
11 a. Stickney, J.L.; Rosasco, S.D.; Song, D.; Soriaga, M.P.; Hubbard, A.T. Surf. Sci. 130, 326, (1983).
b. Hubbard, A.T.; Stickney, J.L.; Rosasco, S.D.; Soriaga, M.P.; Song, D. J. Electroanal. Chem. 150, 165, (1983).
c. Stickney, J.L.; Rosasco, S.D.; Hubbard, A.T. J. Electrochem. Soc. 131, 260, (1984).
12 a. Lu, F.; Salaita, G.N.; Baltruschat, H.; Hubbard, A.T.; J. Electroanal. Chem. 222, 305, (1987).
b. White, J.H.; Abruna, H.D. J. Phys. Chem. 92, 7131, (1988).
13 a. Parratt, L.G. Phys. Rev. 95, 359, (1954).
b. Bommarito, G.M.; M.S. Thesis, Cornell University, 1987.

Figure Legends:

Figure 1 (A) Cyclic voltammogram of the UPD of copper on an iodine covered platinum surface of a Pt/C LSM. (B) same as (A) but for a Pt(111) surface which has been reduced-oxidized through a series of cycles prior to iodine adsorption.

Figure 2.Top panel: X-ray and electrochemical derived isotherms (after rinsing) plotted on an absolute coverage scale after the two data sets were normalized at one point, +0.10 V. Bottom panel: Normalized iodine coverage as a function of applied potential.

Figure 3. XSW fluorescence profiles for both the specular reflectivity and Bragg diffraction regimes for +0.10V and +0.20V after rinsing the electrode surface with clean supporting electrolyte. A magnified view of the Bragg data is show in the insets. Also shown at the bottom, is the complete reflectivity profile. Fits to the data were performed over the entire angular range simultaneously, and are plotted as solid lines.

Figure 4. Same as Figure 3 but at +0.15 V after rinsing, using a Pt/C LSM with a slightly different d-spacing.

Figure 5. Copper concentration profiles after rinsing vs. distance z normal to the LSM's surface, derived from the analysis of the standing wave data. In the main panel all distributions are normalized so that the peak concentration is one. The inset shows the same concentration profiles in terms of their relative areas.

Figure 6 (A) Fractional concentration of surface sites as a function of the distance z, based on the model used to the determine the surface roughness at the platinum/solution interface, and where the z-scale is the same one defined in Figure 5. The area of the Gaussian is normalized to one. (B) and (C) show the variation of the center of mass in the copper distributions of Figure 5, as a function of applied potential and coverage, respectively. The top horizontal dashed line in each panel represents the expected variation in the center of mass for a model in which filling of the bins in (A) is random, whereas the dashed lines at the bottom of (B) and (C) represent the variation expected for a model where the bins in (A) are filled sequentially starting with the deepest one (closest to z=0 Å) first.

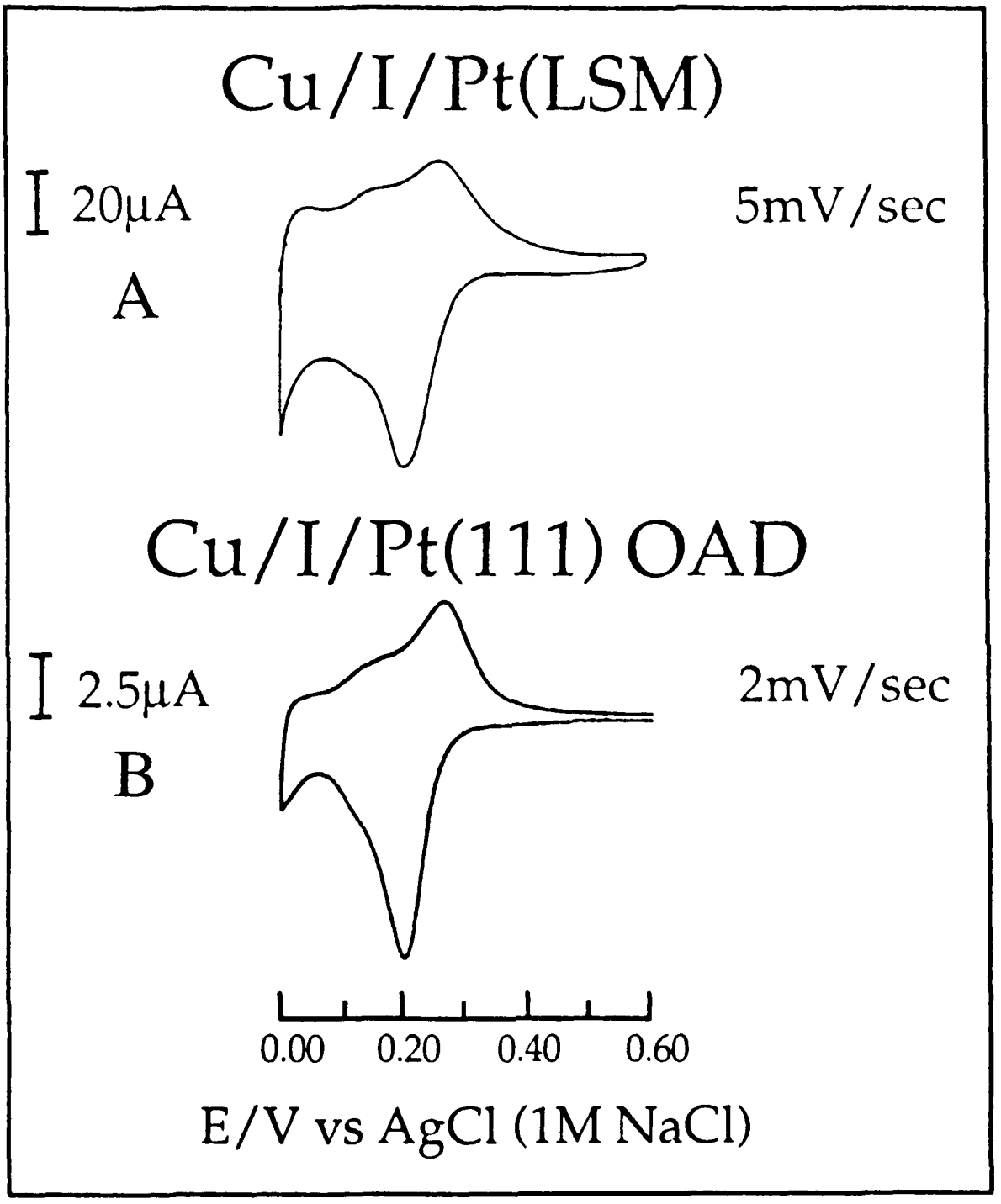
Cu/I/Pt(LSM)
I 20μA
A
5mV/sec
Cu/I/Pt(111) OAD
I 2.5μA
B
2mV/sec
0.00
0.20
0.40
0.60
E/V vs AgCl (1M NaCl)

Figure 1

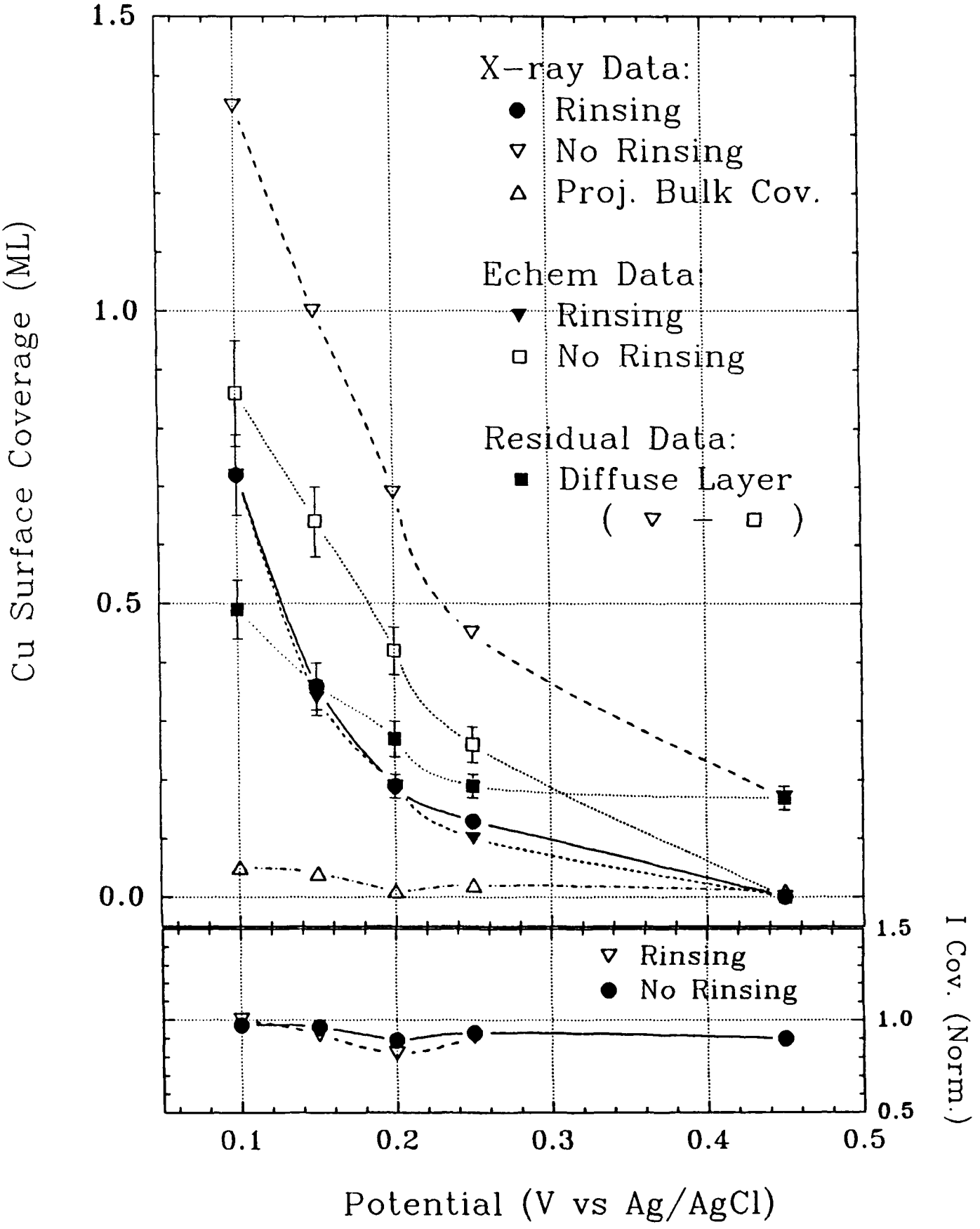
X-ray Data:
Rinsing
No Rinsing
Proj. Bulk Cov.
Echem Data:
Rinsing
No Rinsing
Residual Data:
Diffuse Layer
(▽ − □)
Cu Surface Coverage (ML)
1.5
1.0
0.5
0.0
Rinsing
No Rinsing
I Cov. (Norm.)
1.5
1.0
0.5
0.1
0.2
0.3
0.4
0.5
Potential (V vs Ag/AgCl)

Figure 2

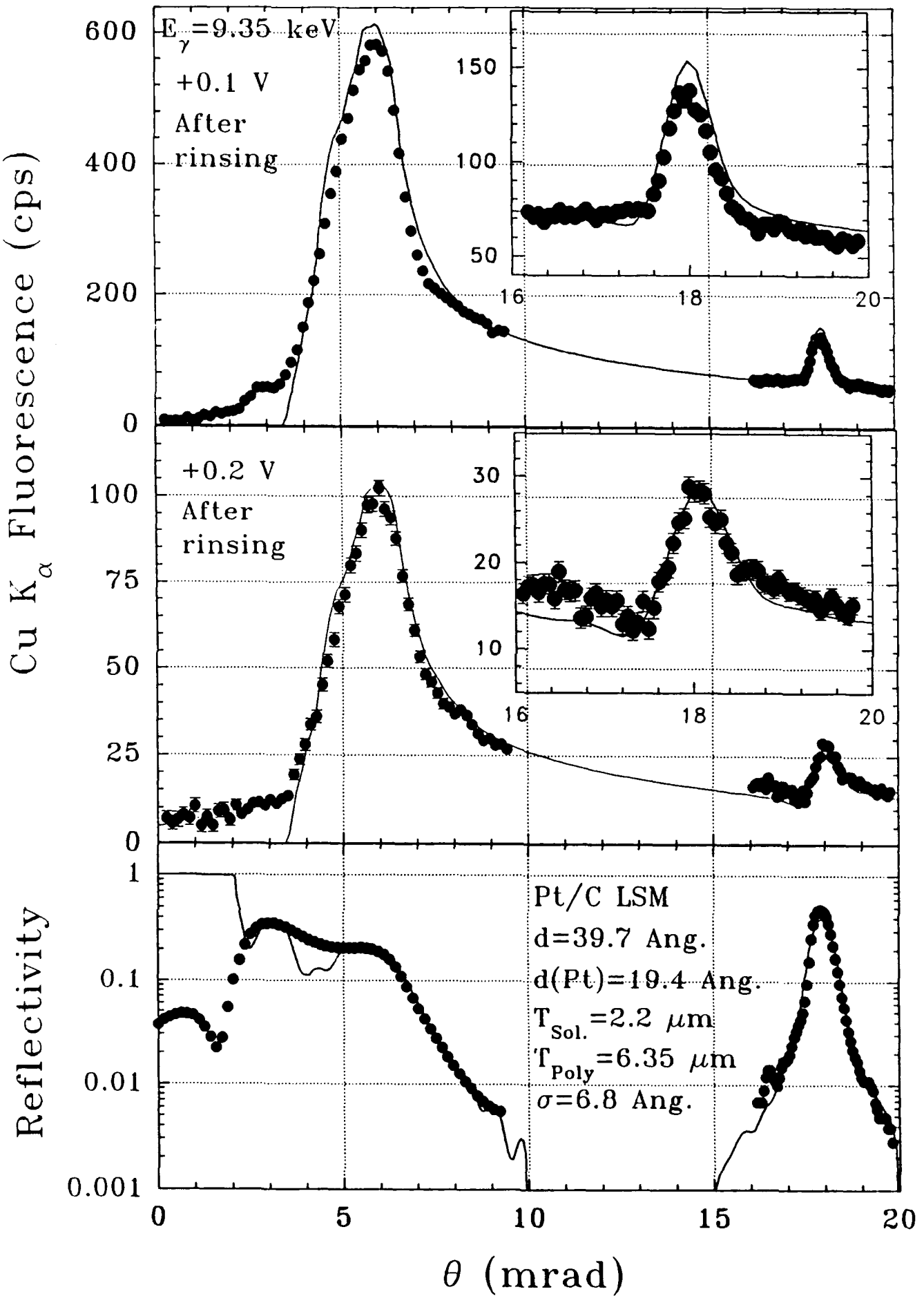
E_γ=9.35 keV
+0.1 V
After
rinsing
+0.2 V
After
rinsing
Pt/C LSM
d=39.7 Ang.
d(Pt)=19.4 Ang.
$T_{Sol.}$=2.2 μm
T_{Poly}=6.35 μm
σ=6.8 Ang.
Cu K_α Fluorescence (cps)
Reflectivity
θ (mrad)

Figure 3

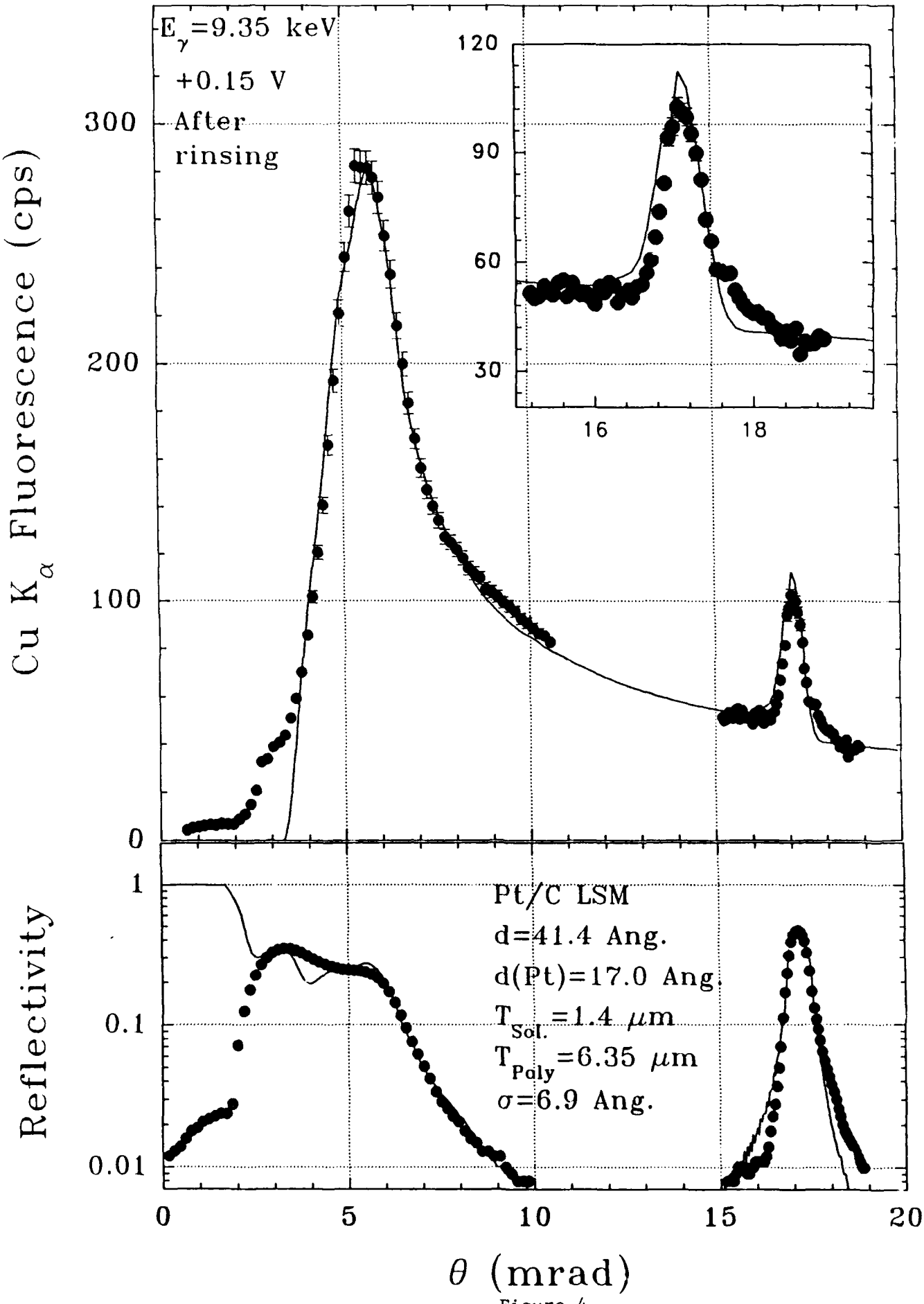
E$_\gamma$=9.35 keV
+0.15 V
After
rinsing
Cu K$_\alpha$ Fluorescence (cps)
300
200
100
0
120
90
60
30
16
18
Reflectivity
1
0.1
0.01
Pt/C LSM
d=41.4 Ang.
d(Pt)=17.0 Ang.
T$_{Sol.}$=1.4 μm
T$_{Poly}$=6.35 μm
σ=6.9 Ang.
0
5
10
15
20
θ (mrad)

Figure 4

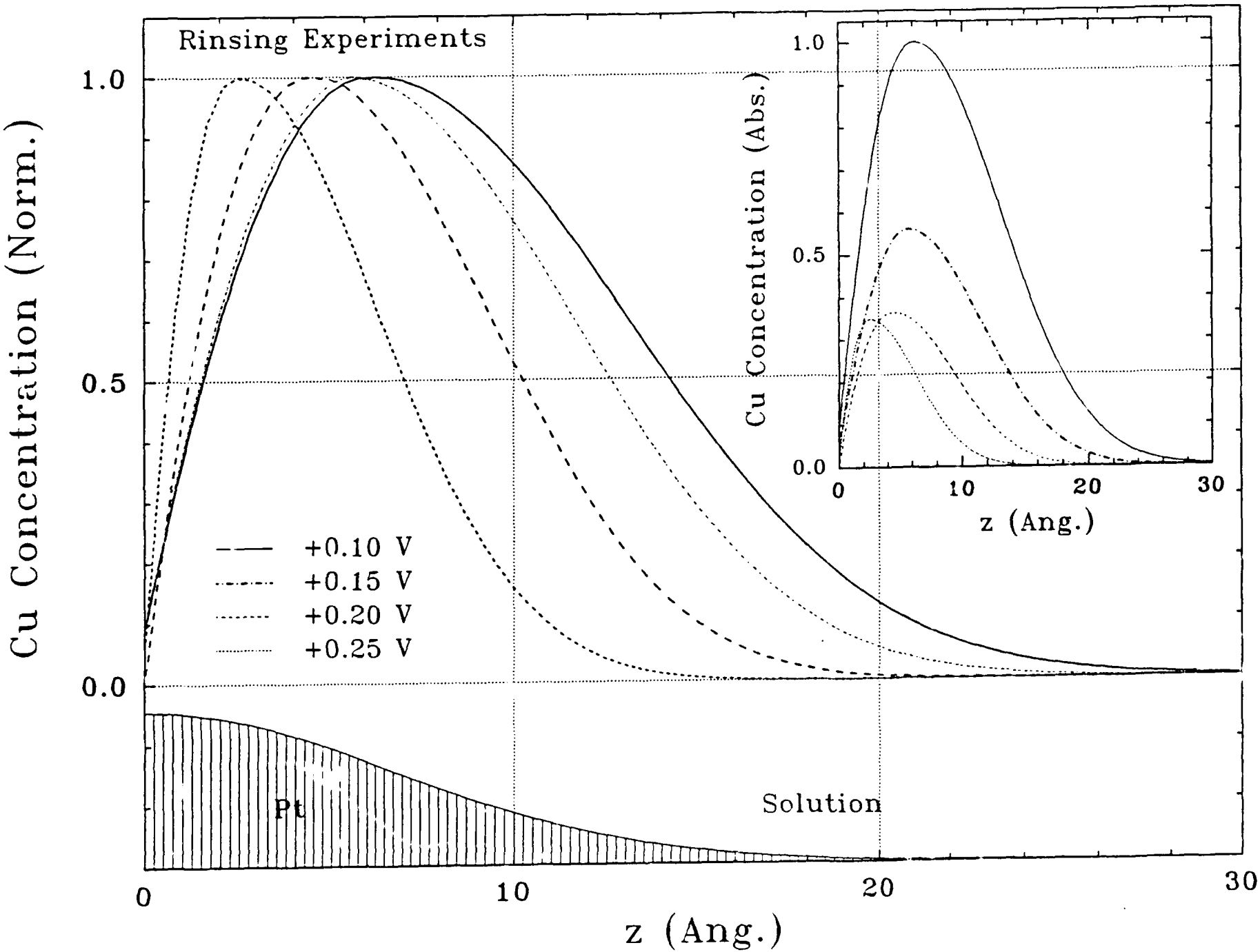
Rinsing Experiments
Cu Concentration (Norm.)
1.0
0.5
0.0
+0.10 V
+0.15 V
+0.20 V
+0.25 V
Pt
Solution
0
10
20
30
z (Ang.)
Cu Concentration (Abs.)
1.0
0.5
0.0
0
10
20
30
z (Ang.)

Figure 5

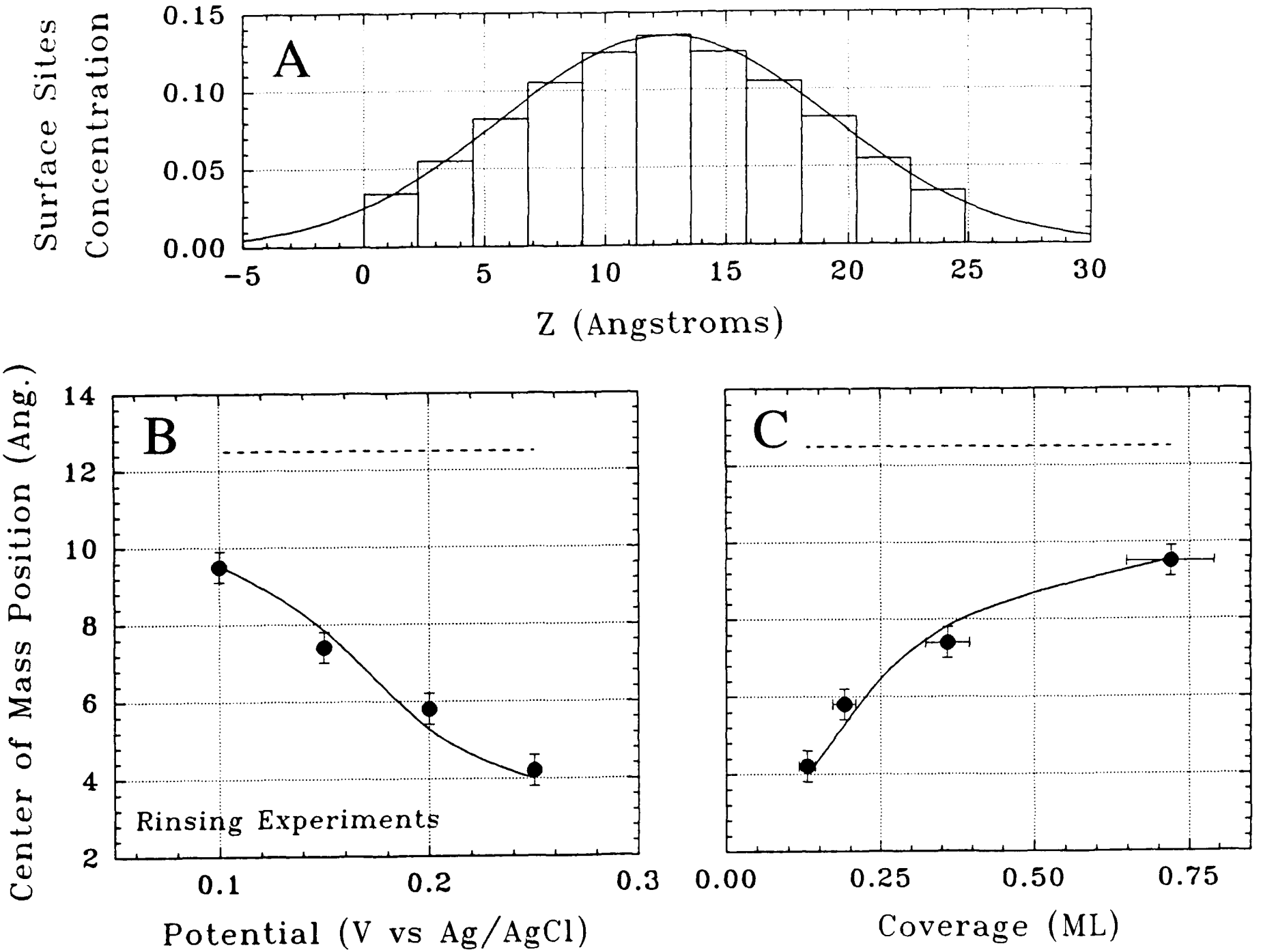
A
Surface Sites Concentration
0.15
0.10
0.05
0.00
−5
0
5
10
15
20
25
30
Z (Angstroms)
B
Center of Mass Position (Ang.)
14
12
10
8
6
4
2
Rinsing Experiments
0.1
0.2
0.3
Potential (V vs Ag/AgCl)
C
0.00
0.25
0.50
0.75
Coverage (ML)

Figure 6